DOI 10.1590/s1982-21702024000100010

ORIGINAL ARTICLE

Groundwater storage dynamics in the Lake Chad Basin revealed by GRACE and a multi-sensor signal separation approach

Marie Grâce Mutimucyeye[1,2,3] - ORCID: 0009-0007-6947-4959

Annoncée Mukeshimana[2] - ORCID: 0009-0001-0245-0991

Jean Pierre Munyaneza[2] - ORCID: 0009-0008-5801-8162

Irène Rwabudandi[3] - ORCID: 0009-0005-1702-3211

Marie Jeanne Nyiransabimana[3] - ORCID: 0009-0000-0567-7211

Janvière Uwamariya[1] - ORCID: 0009-0005-1775-6642

[1] Rwanda Polytechnic, Ngoma College, Civil Engineering Department, Ngoma, Rwanda.
E-mail: mutimucyeyemariegrace@gmail.com; uwajanv91@gmail.com

[2] ULK Polytechnic Institute, Civil Engineering Department, Kigali, Rwanda.
E-mail: mukeshimana.annoncee@ulk.ac.rw; munyaneza.jeanpierre@ulk.ac.rw

[3] University of Rwanda, College of Science and Technology, Civil Environmental and Geomatics Engineering Department, Kigali, Rwanda.
E-mail: iredandi@gmail.com; nyiransabimanam@gmail.com

Received in 26th January 2024.
Accepted in 28th April 2024.

Abstract:

Groundwater resources, a crucial water supply in the Sahel regions of northern Africa, have to be evaluated to ensure its sustainability. In the last decade, Lake Chad Basin (LCB), experienced extreme variabilities in the surface water, which impacted groundwater levels as studied by different authors. Consequently, evaluating the modes of variability of each compartment of the terrestrial water storage (TWS) plays an essential role in LCB water resources management. Therefore, the main objective of this study is to invert groundwater storage (GWS) over LCB using surface water storage (SWS) derived from satellite altimetry and imagery, soil moisture storage (SMS) from the Global Land Data Assimilation System hydrological model (GLDAS), and TWS inferred from Gravity Recovery and Climate Experiment (GRACE) measurements. Here we apply a proper signal separation approach to extract GWS from TWS, which is taken as observations in a least-squares sense to reconstruct GWS. The analysis of the reconstructed GWS series using correlation coefficient, root-mean-square error, and the Nash-Sutcliffe efficiency, shows an improvement of 114%, 26%, and 147%, respectively, compared to the GRACE-based results. These findings could be crucial in the surface and sub-surface water management over LCB.

Keywords: GRACE, groundwater, hydrological model, Lake Chad Basin, signal separation.

How to cite this article: MUTIMUCYEYE MG, MUKESHIMANA A, MUNYANEZA JP, RWABUDANDI I, NYIRANSABIMANA MJ, UWAMARIYA J. Groundwater storage dynamics in the Lake Chad Basin revealed by GRACE and a multi-sensor signal separation approach. *Bulletin of Geodetic Sciences*. 30: e2024010, 2024.

1. Introduction

Groundwater, as the water stored beneath Earth's surface in soil and porous rock aquifers, accounts for as much as 33% of total water withdrawals worldwide, and groundwater resources are under stress due to the pressures of climate change, population growth, salinization, contamination, and rapid depletion (Famiglietti 2014). In fact, to make observations of groundwater levels is difficult and expensive; therefore, understanding groundwater systems is complicated Tregoning et al. (2012). In many regions around the world, groundwater is often too poorly monitored and managed, especially in the developing world, where the supervision is often non-existent. Furthermore, groundwater level data across Africa is scarce and it is difficult to access them due to the absence of centralized databases (Bonsor and MacDonald 2011). Moreover, the estimation of large-scale water balance using these limited ground-based measurements is inaccurate and are prone to errors of all sorts.

The Gravity Recovery and Climate Experiment (GRACE) observations have been used to map the monthly changes in terrestrial water storage (TWS) at regional to global scales. TWS refers to the total amount of water stored on the Earth's land surface and subsurface. The main components of TWS include soil moisture storage (SMS) - the water stored in the unsaturated zone of the soil, groundwater storage (GWS) - the water stored in the saturated zone below the water table, surface water storage (SWS) - the water stored in lakes, rivers, and wetlands, snow and ice, and biomass water - the water stored in living vegetation, such as trees, shrubs, and crops. Previous investigations (cf. Rodell et al. 2009)consuming groundwater faster than it is naturally replenished and causing water tables to decline unremittingly. Indirect evidence suggests that this is the case in northwest India, but there has been no regional assessment of the rate of groundwater depletion. Here we use terrestrial water storage-change observations from the NASA Gravity Recovery and Climate Experiment satellites and simulated soil-water variations from a data-integrating hydrological modelling system to show that groundwater is being depleted at a mean rate of 4.0 1.0 cm yr-1 equivalent height of water (17.7 4.5 km 3 yr-1 revealed that there is potential to separate the different components of the GRACE signal using ancillary datasets to estimate GWS based on GRACE-derived TWS. Groundwater estimation based on GRACE-derived TWS relies on the mass conservation approach, at which TWS can be disaggregated into its sub-domain.

In the Lake Chad Basin (LCB), where water resources are crucial for sustaining livelihoods and ecosystems, there is a critical need to comprehensively assess groundwater storage alongside surface water dynamics to ensure sustainable water management and resilience in the face of environmental changes. Previous studies examined the water storage variability of LCB by applying remotely sensed and modeled datasets e.g., Alla et al. (2019) but they did not consider the resolution dissimilarity of satellite data products (i.e., gravimetric, altimetry, and imagery datasets) and an improved signal separation approach. The present study applies an approach called point-mass modeling (Baur and Sneeuw 2011), which is considered a radial basis function to forward and invert all datasets aiming at matching their different resolutions with that of GRACE, and use of Principal Component Analysis (PCA) for decomposition of each component of TWS (Jolliffe 2000). The SWS, SMS, and GWS are fitted to the GRACE-derived TWS by applying a "tie-in "method proposed by Ferreira et al. (2020a). Specifically, the aims of this study are to (i) provide the same radial basis function for advancing and reversing the gravitational potential considering each component of the TWS budget, and (ii) apply a signal separation approach for improving the estimation of groundwater storage.

2. Regional setting

The LCB is located between latitudes 6° and 24°N, and longitudes 7° and 24° E and covers 2,397,424 km^2. The southern part of the basin is made of three aquifers stated as the upper, middle and lower aquifers and are shared

by five countries bordering the Lake Chad namely Niger, Chad, Cameroon, Central Africa Republic and Nigeria. The Lake Chad (Figure .1) lies at an altitude of about 283 m above mean sea level on the border of the Sahara between latitudes 12° N and 14° N and longitudes 13°E and 15° E. It is hydrologically closed, and occupies less than 1% of the geographical drainage basin, and has an average depths varying between 1.5 and 5 m (Odada et al. 2003).

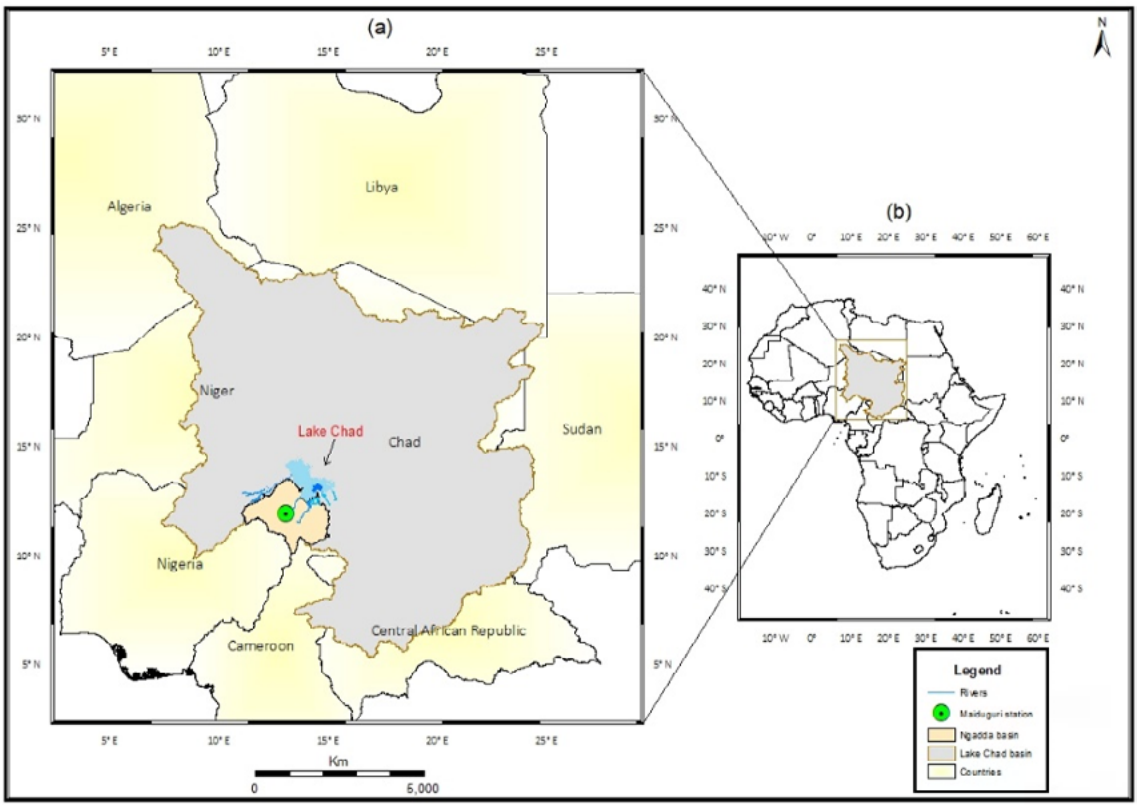

Figure 1. (a) Lake Chad Basin's geographical location with its eight riparian countries, which share the interest from the basin, and Lake Chad with a small surface of water in its Southern part. Panel (a) also shows Ngadda Basin where the available in situ data were collected in Maiduguri station, shown in a green point. Panel (b) shows physical delimitations of Lake Chad Basin on the map of Africa.

3. Materials and Methods

3.1. Datasets

3.1.1. Satellite altimetry-imagery derived surface water storage

Datasets were acquired from sensors Landsat 7 ETM+ and Landsat 8 OLI, which have spatial and temporal resolutions of 30 m and 16 days respectively, and were used to extract the surface area for the lake investigated. The data were downloaded from USGS Earth Explorer (http://earthexplorer.usgs.gov/) with cloud cover range less than 20%, and paths/rows of 184/51, 185/50, 185/51 and 186/50 which were mosaicked to get a full image. A total of 171 images were downloaded from April 2002 to June 2017, but only 79 Landsat clear images were processed. They were used for surface water estimation by applying case dependent thresholds. Time series of monthly lake level height variations computed from TOPEX/POSEIDON (T/P), Jason-1 and Jason-2, provided by United states Department of Agriculture (USDA) available on (https://ipad.fas.usda.gov/cropexplorer/global_reservoir/), covering

the same period have been smoothed with a median type filter in order to eliminate outliers and reduce high frequency noise. The relationship between area and elevation was estimated by using a linear regression model, pairing up the computed surface area with their corresponding satellite altimetry heights in a scatter plot. The area-elevation relationship (cf. Ferreira et al. 2018)Niger, and Senegal Basins of West Africa was investigated. An altimetry-imagery approach was proposed to deduce the contribution of Lake Volta to TWS as \"sensed\" by GRACE. The results showed that from April 2002 to July 2016, Lake Volta contributed to approximately 8.8% of the water gain within the Volta Basin. As the signal spreads out far from the lake, it impacts both the Niger and Senegal Basins with 1.7% (at a significance level of 95% was then used for making provisions for the missing months of Landsat data for the entire study period, from April 2002 to June 2017.

3.1.2. GRACE Level-2 data

GRACE satellite missions are the only geodetic remote sensing technology currently available for measuring water stored below the first few centimeters of the soil column, down to deep aquifers and the total liquid and frozen water storage. In this study, the spherical harmonic coefficients were derived from GRACE data, Center for Space Research (CSR) of University of Texas, United States of America (USA). According to (Swenson and Wahr 2006) these errors manifest themselves in maps of surface mass variability as long, linear features generally oriented north to south (i.e., stripes, high degree of spatial correlation exists in GRACE errors and behaves as long as south-north linear features which is called “stripes”. In order to reduce these errors, de-correlation procedure is conducted according to Duan et al. (2009). Besides the stripes error, high degree spherical harmonic coefficients still include large errors, thus smoothing is still needed while using them to estimate mass changes (Swenson and Wahr 2006) these errors manifest themselves in maps of surface mass variability as long, linear features generally oriented north to south (i.e., stripes. In their studies, Forsberg et al. (2017) and (Baur and Sneeuw 2011) did not apply smoothing and filtering to the Stokes coefficients. Furthermore, Jacob et al. (2012), applied the stripe step in their mascon solutions based on the Stokes coefficients, hence improving the sample characteristics of the estimated mascon.

3.1.3. Modeled data from GLDAS and WaterGAP

GLDAS adopts four land surface models to produce different fields of the land surface as reported by Ayman and Shuanggen (2014). The data are available from the Goddard Earth Sciences Data and Information Services Center (GES DISC). In this study, Noah 0.25°x0.25° grid data covering the period from April 2003 to June 2017 were used. The WaterGAP Global Hydrological Model (WGHM) belongs to the Water-Global Assessment and Prognosis (WaterGAP) model Alcamo (2010)which consists of two main components-a Global Water Use model and a Global Hydrology model. These components are used to compute water use and availability on the river basin level. The Global Water Use model consists of (a and it accounts for four of the most important continental water storage components. The model is developed at the University of Kassel and the University of Frankfurt in Germany. rendering water management difficult and unreliable. This study analyzes the changes in the hydrological behavior of the Lake Chad basin with extreme climatic and environmental conditions that hinder the collection of field observations. Total water storage (TWSIn this research, the groundwater fields induced from the new version of the WaterGAP, (version 2.2d) were used for estimating GWS based on GRACE data. The monthly groundwater storage fields from the WaterGAP covers a period from April 2003 till June 2017 with a spatial resolution of 0.5°.

3.1.4. In-situ Groundwater Series

The data was collected from Maiduguri station (Ngadda catchment located in LCB) and exhibits only one set of in-situ groundwater time series data covering the period from April 2006 to December 2009. The area of Ngadda catchment is composed of two basins, that is, Ngadda basin (42,535 km2) and Magay basin (36,893 km2) in the southwest region of the Lake Chad (Figure 1). The dataset was digitally reconstructed from the time-series available in Ref. Alla et al. (2019) using the Digitize It digitizer software (Bormann 2016). Next, it was necessary to normalize

the extracted time series by using their respective standard deviation so that the findings could not be impacted by the unknown specific yields. Due to the missing periods occurred in 2009, linear interpolation was carried out to fill the gaps in the in-situ GWS series. After that, the series of data were used for validation of groundwater storage over Ngadda Basin in LCB.

3.2 Methodology

3.2.1 The Inverse Point-mass Approach

The technique of point-mass modeling has been used by Baur and Sneeuw (2011) for water mass inversion using GRACE datasets. The gravitational potential derived from GRACE data is used as observations in the inversion scheme Ferreira et al. (2020a, 2020b). The estimated point-mass variations from GRACE-derived gravity changes exhibit greater similarity to mass concentrations (mascons) from local GRACE K-band range and range rate data Luthcke et al. (2006).

The gravitational potential is calculated using Newton's integral for infinitesimal surface elements as (cf. Ferreira et al. 2020b):

$$\delta V(r,\varphi,\lambda,t) = GR^2\rho_W \sum_k \Delta r\,(t)\Delta\varphi_k\Delta\lambda_k \frac{cos\,\varphi_k}{\ell_k} \quad (1)$$

where G is the Newton's gravitational constant (6.67259 x $10^{-11}m^3kg^{-1}s^{-2}$), R is the radius of the Earth, ρw is the density of freshwater (which can be considered constant: $1000kg/m^3$),.and ℓ_k is the distance between the computation point defined by the geocentric coordinates (r, φ, λ) and the running point defined by the geocentric coordinates at the center of a given spherical panel k.The Earth's surface was subdivided into 41,334 equal-area cells or pixels (White et al. 1992, Mahdavi-Amiri et al. 2015). The functional model of the least-squares problem is truncated at the same spectral resolution as the gravitational potential calculated using spherical harmonic synthesis to address spectral inconsistencies (Ferreira et al. 2020a).

The undetermined parameters (apparent water thickness) are estimated using a regularized minimization approach, known as Tikhonov regularization (Hansen 2000). The optimal regularization parameter is determined using the L-curve criterion, which provides a good balance between the solution norm and residual norm (Baur and Sneeuw 2011, Wu et al. 2018). The observations, that is, the right-hand side of Eq. (1), were generated using the spherical harmonic synthesis based on the GRACE Stokes's coefficients described in Sub-section 3.1.2. For further details about this procedure, refer (Wahr et al. 1998, Baur and Sneeuw 2011, Ferreira et al. 2020a).

Leakage effects, where signals spread spatially and are not concentrated directly over the area of mass variation, are a major challenge (Baur et al. 2009). The approach proposed by Tang et al. (2012)is used to correct for leakage effects, which relies only on GRACE data and can be applied globally. The apparent water thickness obtained from GRACE harmonic solutions is compared with the land surface densities to discern between the two and correct for leakage (Wahr et al. 1998).

3.2.2 GRACE-derived groundwater storage

Building upon previous work, researchers have employed various statistical-based approaches to analyze GRACE-TWS data. For instance, Forootan et al. (2014) carried out a statistical-based model to support TWS analysis, considering groundwater storage, which had been omitted in their previous work. The procedure prioritized the spatial patterns of terrestrial and water storage changes to make a correct separation of the TWS main sub-domains. Similarly, Ndehedehe et al. (2016) used a statistical analysis of GRACE-derived TWS, building on the work of Schmeer

et al.(2012), who had decomposed the mass signals within GRACE monthly gravity fields into the main time-varying components of the Earth's gravity fields, including atmosphere, ocean, and continental hydrology.

Ferreira et al.(2020a) proposed a method based on PCA that takes into account groundwater storage by considering the Empirical Orthogonal Functions (EOFs) of groundwater storage from a hydrological model as an initial guess. This "tie-in" approach seeks to integrate the sub-domains of the TWS, coming from different satellites, as described in the TWS-budget equation (Eq. 2).

$$\mathrm{TWS} = \mathrm{GWS} + \mathrm{SMS} + \mathrm{SWS} + \mathrm{SWE} \tag{2}$$

In Eq. (2), SWE is disregarded and assumed to be zero in this study due to the absence of snow in the Sahel regions in Africa. Therefore, it is possible to estimate GWS from GRACE-TWS using Eq. (2), hereafter named the TWS-budget equation, given the soil moisture storage (SMS) retrieved from a hydrological model and the surface water storages (SWS) derived by satellite altimetry and imagery.

In the "tie-in" approach, the water storage given by Eq. (2) can be decomposed as (Ferreira et al. 2020a):

$$\mathrm{T}=\mathrm{c}_G\mathrm{V}_G{}^T+\mathrm{c}_S\mathrm{V}_S{}^T+\mathrm{c}_I\mathrm{V}_I{}^T+\mathrm{c}_C\mathrm{V}_C{}^T+\mathrm{c}_R\mathrm{V}_R{}^T \tag{3}$$

where c and V are matrices with dimensions $t\,x\,k$ and $n\,x\,k$ expressing the series coefficients that stand for the temporal evolution (i.e., the principal components – PCs) and the orthonormal spatial base functions standing for the spatial patterns (i.e., EOFs), respectively. As the GLDAS-Noah is the provider of the water stored in soil, canopy, and ice/snow, for the study area in this research, only soil moisture storage is available because in this region, there is no ice and snow, and canopy water is negligible. Thus the Eq. (3) can be reduced as:

$$\mathrm{T} = \mathrm{c_G}\mathrm{V_G}{}^{\mathrm{T}} + \mathrm{c_S}\mathrm{V_S}{}^{\mathrm{T}} + \mathrm{c_R}\mathrm{V_R}{}^{\mathrm{T}} \tag{4}$$

where S represents the SMS obtained from GLDAS-Noah hydrological model, while R stands for inland reservoir given here as SWS.

The coefficients c_G, c_S, and c_R appearing in Eq. (4) can be estimated by least squares given the observations ${}_nL_t = T^T$, that means the GRACE-derived TWS fields and a priori information for each variable defining the components of the "TWS-budget" as provided by Eq. (2). It is significant that the first term in the right-hand side of Eq. (4) has not been considered by Forootan et al. (2014) as their contributions deals with the reconstructions of TWS provided by GLDAS-SMS and SWS. Therefore, to estimate the coefficient of each water storage compartment of the TWS-budget equation, the least-squares problem defined as:

$$\mathrm{X} = (\mathrm{J}^T\mathrm{WJ})^{-1}\mathrm{J}^T\mathrm{WL} \tag{5}$$

can be utilized here for those coefficient estimations and it is given by X with dimension $K\,x\,t$. The matrix J, an $n\,x\,K$ is the coefficient matrix in which K is the total number of considered modes to be estimated by accounting the individual variables in Eq. (4). It means that the K is equal to the summation of the number of modes to compress groundwater (K_G), the number of modes for GLDAS-Noah soil moisture (K_S) and the number of modes of inland reservoirs(K_R).

Finally, the reconstructed groundwater storage ($\widehat{\mathbf{G}}$) is given as (Ferreira et al. 2020a):

$$\hat{G} = \widehat{C_G}V_G^T \tag{6}$$

where $\hat{\mathbf{c}}_\mathrm{G}$ is the estimated PCs for the groundwater storage from Eq. (5) and V_G.

The herein used approach is different from the one called signal separation because its intention is to adjust the sub-domains appearing in the TWS-budget equation such as GWS, SMS and SWS to TWS, which is considered

as observation; that is why it is termed as the “tie-in” approach by (Ferreira et al. 2020a). Thus, there is a difficult here as the temporal (PCs) and spatial (EOFs) patterns of groundwater fields, none of them is available since they are unknown in the problem. Therefore, the $WGHM$ modeled GWS was regarded to provide the available datasets so that the preliminary approximation for the GWS can be found. Exactly, the GWS fields gained from $WGHM$ hydrological model (Section 3.1.3) were applied. Furthermore, it was also used for comparing its variations with the one of the computed from Eq. (2).

4. Results and Discussions

4.1 Inversion and Decomposition of Different Water Storage Components

The first goal of this research was to explore a method that allows the integration of GRACE observations, satellite altimetry and satellite imagery considering their respective spatial resolutions. The applied method was based on the point-mass modelling approach, which was accounted for inverting GRACE synthesized gravitational potential at the satellite orbits into TWS fields at the surface of the Earth. Afterwards, the point-mass modelling was considered for forwarding the gravitational potential at GRACE’s orbit due to the soil moisture storages and surface water storages, where every single inverted component of the TWS-budget (i.e., GWS, SMS and SWS) covering the entire LCB was summarized using PCA decomposition, which result to the spatial patterns (i.e., EOFs) and temporal patterns (i.e., PCs).

Satellite altimetry-imagery data were used to provide SWS of Lake Chad in terms of monthly field as reported in (Ferreira et al. 2018, 2020a)Niger, and Senegal Basins of West Africa was investigated. An altimetry-imagery approach was proposed to deduce the contribution of Lake Volta to TWS as \”sensed\” by GRACE. The results showed that from April 2002 to July 2016, Lake Volta contributed to approximately 8.8% of the water gain within the Volta Basin. As the signal spreads out far from the lake, it impacts both the Niger and Senegal Basins with 1.7% (at a significance level of 95%, who applied a linear model while predicting the surface area and water level of the missing months for Volta and Yangtze River basins respectively. In addition, having the surface area and water level series of Lake Chad and by considering the pairs of area and elevation of the current month and the preceding one, it was feasible to compute the water volume variations.

The results revealed that there is a high variability of water volume due to the surface changes as it was confirmed by Buma and Lee(2016)rendering water management difficult and unreliable. This study analyzes the changes in the hydrological behavior of the Lake Chad basin with extreme climatic and environmental conditions that hinder the collection of field observations. Total water storage (TWS who found that the water volume stored in LCB is solely governed by the surface water of the lake. The point-mass modelling was assumed to represent the surface masses at each grid cell covering the entire surface of the Earth. However, due to the spectral incompatibilities between each of the datasets and GRACE, which was expanded up to degree and order 96, the filter of the model was considered by using the decomposition of the reciprocal distance. Since the given satellite altimetry-imagery and modelled products are not spectrally consistent with GRACE products, the inverse modelling was applied to set all observations at the same spectral resolution. To synthesize the gravitational potential on a grid with 3-by-3 arc-degree at 500 km altitude, the spherical harmonic synthesis (cf. Ferreira et al. 2020a)was applied given the CSR-derived GRACE harmonic solutions up to degree and order 96. The nominal resolution of GRACE data is rather considered as 3-arc -degree.

PCA was used to identify the dominant spatiotemporal patterns of GWS, TWS, SMS and SWS. For statistical inference, each TWS sub-domain was decomposed into sets of principal components (PCs, i.e., temporal patterns)

and their associated empirical orthogonal functions (EOFs, i.e., spatial patterns). The greatest values of PCs were used to measure and make it unitless while the EOFs were measured by the greatest values of their associated PCs so that the anomaly maps of water storage could be represented in mm.

Figure (2) shows the loadings for the first four modes of SWS, demonstrating the temporal patterns (i.e., PCs) along with their corresponding spatial patterns known as EOFs. The total variance of SWS is almost 100 % and the minimum and maximum range of surface water storage is between 0 and 100 mm respectively.

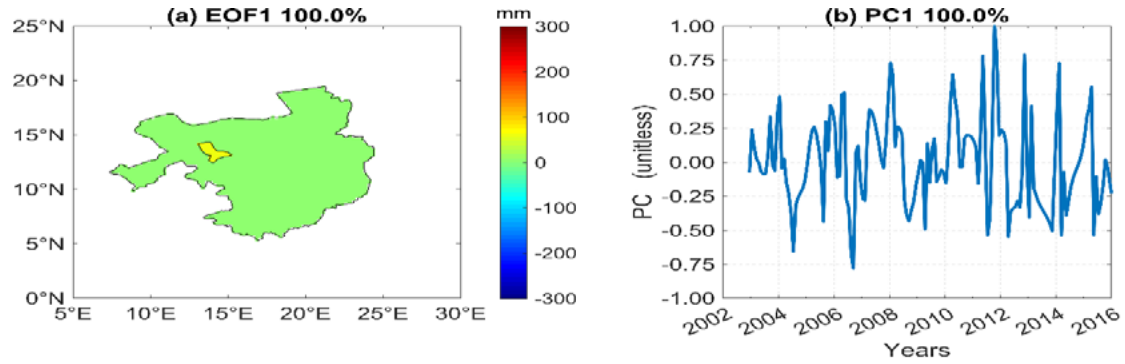

Figure 2: PCA decomposition of SWS variations over Lake Chad Basin. The EOF and PC are loadings showing spatial and temporal patterns variations of SWS respectively.

In regards to the GLDAS-SMS, the PCA loadings are described in Figure (3) where the first four modes explained 94.5% of the total variance. The most dominant mode was the first one with 85.4% of total variability while the second, third and fourth were explained by 5%, 2.6% and 1.5% respectively.

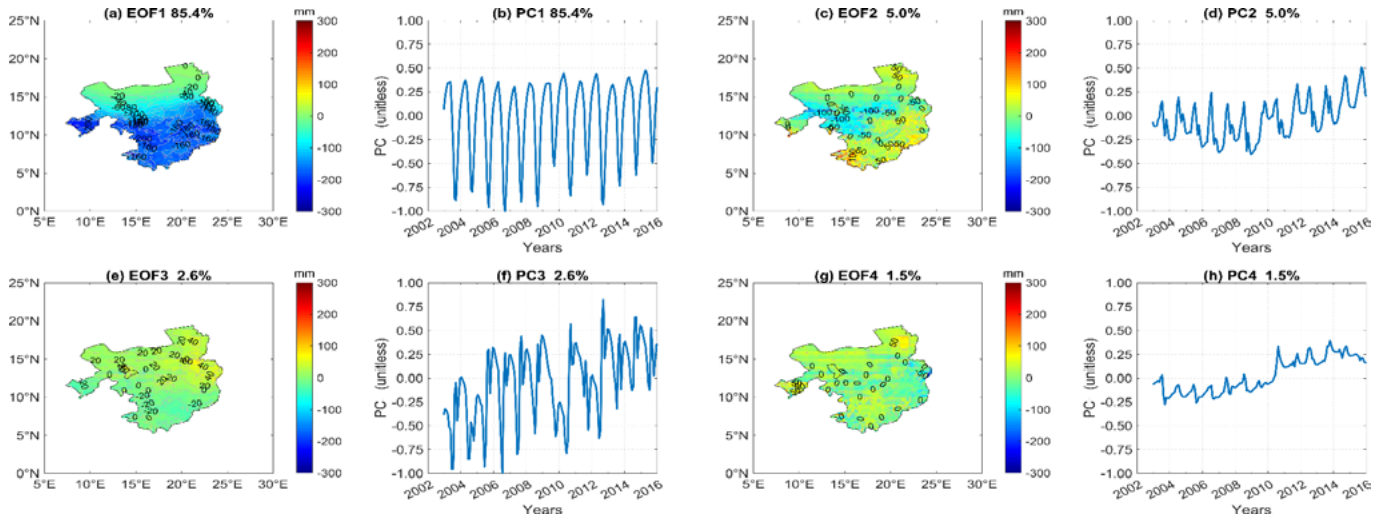

Figure 3: PCA of GLDAS-SMS variations over Lake Chad Basin in which the panels (a)-(h) hold the EOFs and their respective PCs.

The strong annual variations were depicted by the PC_1 and its associated EOF_1 exhibits the increase in soil moisture wetness from the northern to the southern part of the basin ranging between 0 and -200 mm. Hence, the results on spatial patterns (Figure 3a) explain that the SMS contribution in the LCB is significant with the wetness average of -118 mm. The same analysis was carried out to the total water storage (Figure 4), which is characterized by decrease on water storage from the southern to the northern part of the basin.

The average of TWS wetness accounting for the first mode is almost 145.8 mm. The temporal evolutions were described by high annual variations for the PC_1 and multi-annual variations for the remaining PCs. Thus, the TWS changes depends largely on the river flow from the Chari and Ngadda River systems, however Chari River system is the main source of Lake Chad.

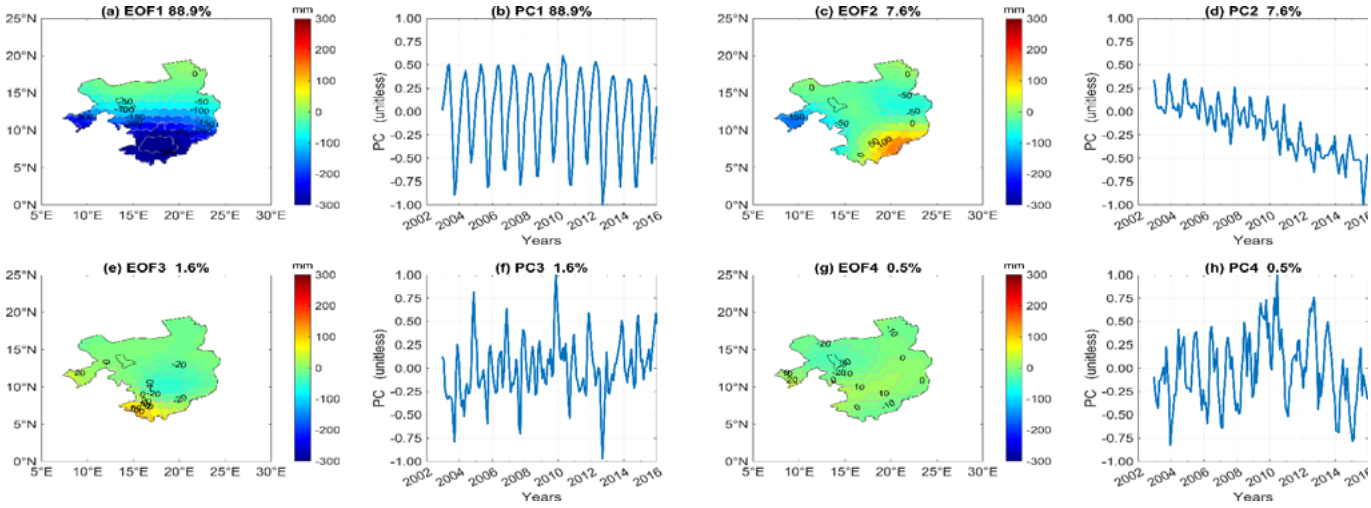

Figure 4: Decomposition of PCA for GRACE-TWS changes over Lake Chad Basin.

Furthermore, groundwater storage was then estimated, given GRACE-TWS, GLDAS-SMS and satellite altimetry-imagery derived SWS. After that, PCA was applied to the resulted GWS, after subtracting SMS and SWS from TWS (Eq. 2). A significant 99.9 % of the total variance was explained by first four modes. At last, Figure 5 shows the PCA decomposition for WGHM derived GWS with a total variance for the first four modes of almost 58.2%. The dominant mode was first one, with a percentage of 41.8%, while second, third and fourth modes explained by 7.5%, 4.8% and 4.1%, respectively, of the total GWS total variability. Figure 5b depicts the dominant annual variations with a peak GWS value at end of 2011 since the remaining temporal patterns, that is, PC_2, PC_3 and PC_4 were characterized by multi-annual variations.

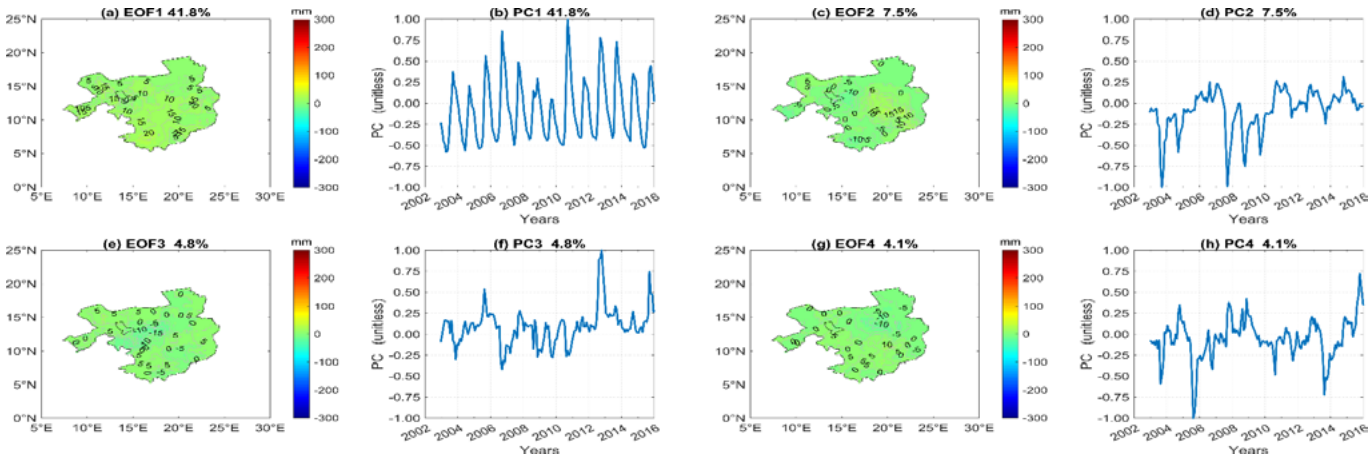

Figure 5: Panels (a)-(h) depict the first four modes of EOFs and PCs resulting from PCA decomposition for WGHM-GWS.

At this site, Döll et al. (2003) confirmed that, in Africa, most of the basins in the north of the equator do not perform well with WGHM output, and LCB is located in this part of Africa. That is why this model did not match well with the results found by Bihn et al.(2020), who confirmed that most LCB's water is stored primarily in groundwater but also in soil moisture. That is, 70% of water storage in this region is generated by sub-surface water.

4.2. Inversion and Reconstruction of Groundwater Storage

In regards to the second topic of this study, a tie-in approach based on principal components and empirical orthogonal functions was applied and used to estimate GWS using multi-satellite missions. This approach was crucial for fitting the temporal patterns of GWS, SMS, and SWS to TWS, which was taken as observations. After that, each component of TWS could be reconstructed using the estimated PCs. The PCA decomposition of each sub-domain was statistically significant since almost the first four PCA modes provided a cumulative variance of about 100% except GLDAS-SMS and WGHM-GWS, which explained less than 99.0% of the total variance. Then, it was required to increase the number of modes, that is, 19 modes for SMS, 124 modes for WGHM-GWS and 1 for SWS, in order to reconstruct the total variance in GRACE-TWS series. Therefore, the total number of modes was 144. Consequently, the tying in the EOFs of each sub-domain of TWS was carried out in a least-square sense. The result was built by the estimated temporal patterns (i.e., PCs), which were used for sub-domains reconstruction.

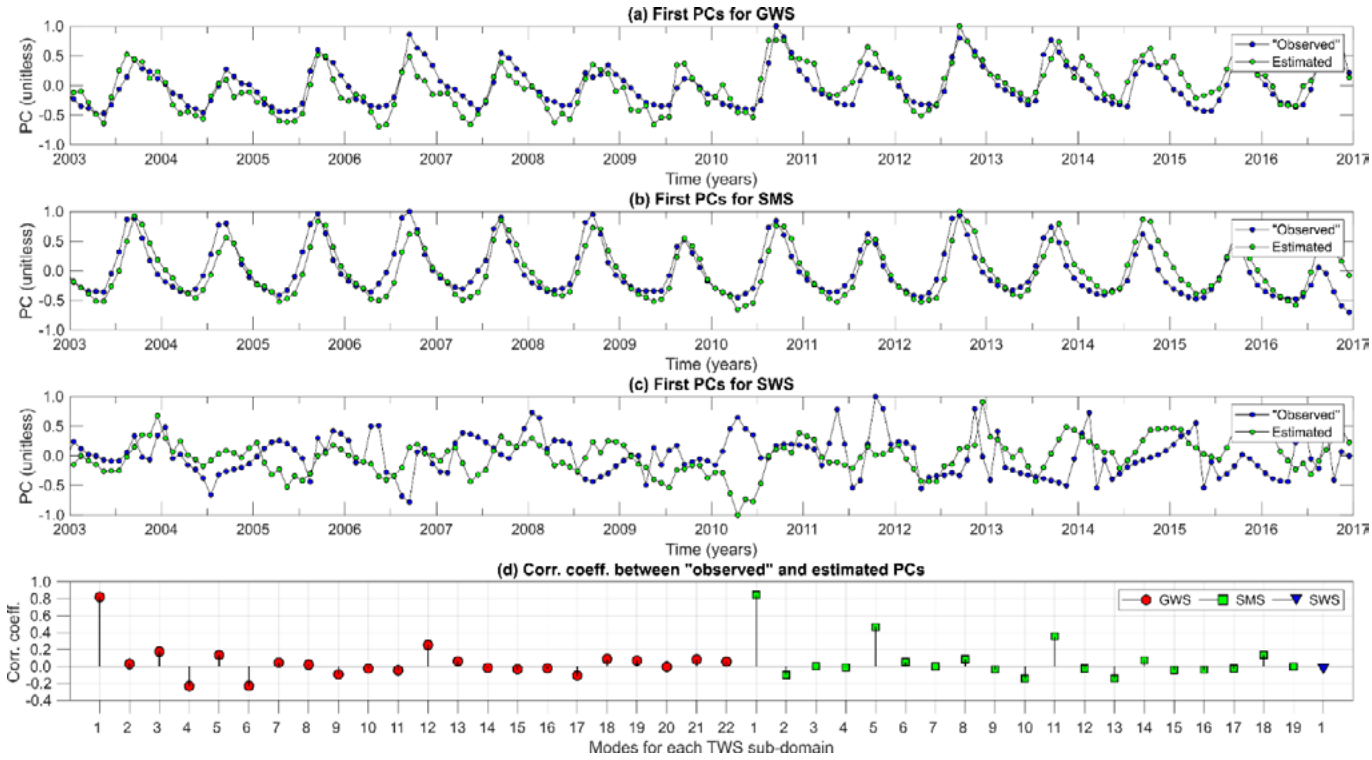

Figure 6: The top-three panels depict the comparisons of the first modes of the "observed" and the estimated PCs for GWS (a), SMS (b) and SWS (c) sub-domains. Panel (d), shows the correlation coefficients between the "observed" PCs and the estimated ones for all sub-domains of TWS.

Figure 6 describes the comparison between the estimated and the "observed" PCs for the first mode where a good agreement was found on GWS and SMS series except slight differences occurred in some years. For instance,

Figure 6a presents some dissimilarities in 2011 and between 2013 and 2015. Concerning the SWS shown in Figure 6c, the compared PCs series are characterized by differences in almost all of the study period except the year of 2003. This is due to the unsubstantial amount of SWS in LCB caused by many factors that occurs in Sahelian zone. Figure 6d explains the coefficient correlation between the "observed" and the estimated PCs for the respective number of modes considered for the corresponding sub-domain, that is, 124 for GWS, 19 for SMS and 1 for SWS). The results revealed that only the first mode presented a strong correlation for GWS, the first and the fifth for SMS while the SWS did not present a sensible value of correlation. Actually, the estimated and observed PCs for GWS and SMS series exhibited a slight difference compared to the ones of SWS, which found insignificant herein and in previous studies such as Alla et al. (2019). Concerning to the results from parameter estimation (i.e., the estimated PCs represented by $\hat{c}_G$), the reconstruction of groundwater fields was performed using Eq. (5). For instance, for reconstructing GWS, the first mode shown in Figure 6a and the correlation between the estimated and the "observed" PCs presented in Figure 6d were used.

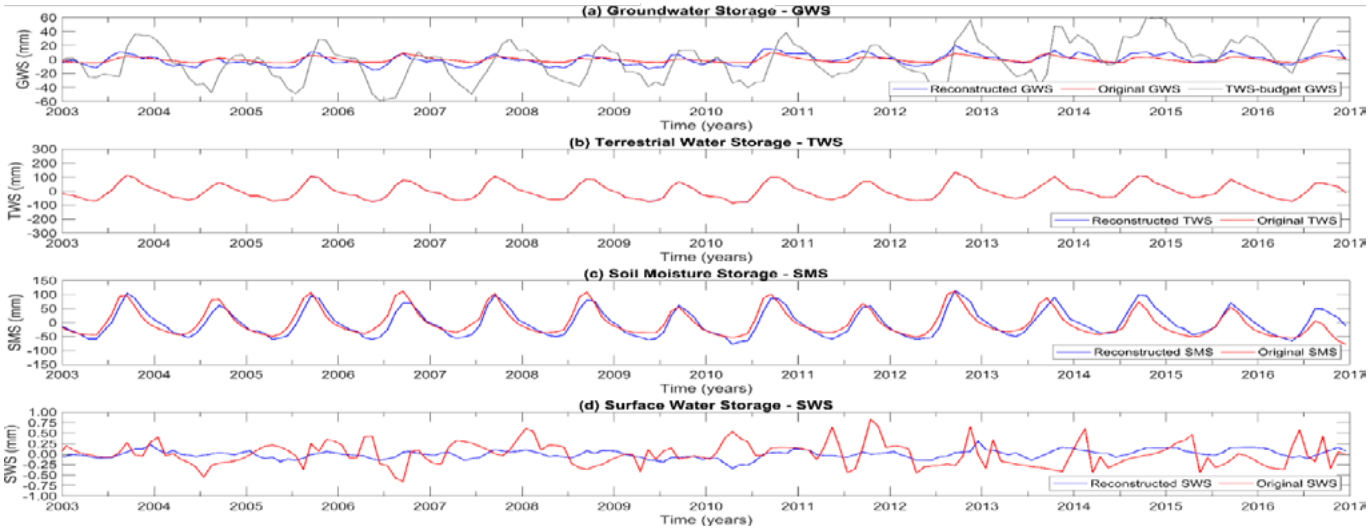

Figure 7: The top-three panels show the assessment between the reconstructed (blue solid line) and the original (red solid line) series of water storage sub-domains and TWS too (b). Panel (a) for GWS, (c) for SMS and (d) for SWS series.

The averaged time series of GWS for LCB was computed by considering the mean of 102 geographical locations and it is displayed in Figure 7a. In regards to TWS (Figure 7b), the reconstructed and the original series presented the same annual variations since TWS was taken as observation in a "tie-in" approach. For SMS shown in Figure 7c, the comparison between the evaluated series presents a relatively good agreement between both series, with the interannual variability in rainy and sunny seasons possibly being the cause of SMS variations in LCB. In regards to SWS (Figure 7d), significant differences are presented in almost all of the study period with multi-annual variations, which could be induced by the long dry season in LCB (Buma et al. 2018).

Furthermore, the annual variations explained by the three series of GWS, could be explained by the variation of rainfall in this basin, which could impact groundwater aquifers too. At this point, the most dominant rainfall occurred between July and September as reported by Alla et al. (2019) . Consequently, the reconstructed GWS series exhibit a significant agreement with the original GWS in terms of water stored in aquifers, which was shown by moderate variations (Figure 8). In regards to GWS series obtained based on Eq. (1), high changes occur in almost all the period of study, compared to the reconstructed and original series. Overall, the reconstructed GWS series presents a better performance than the original and TWS-budget GWS series over LCB.

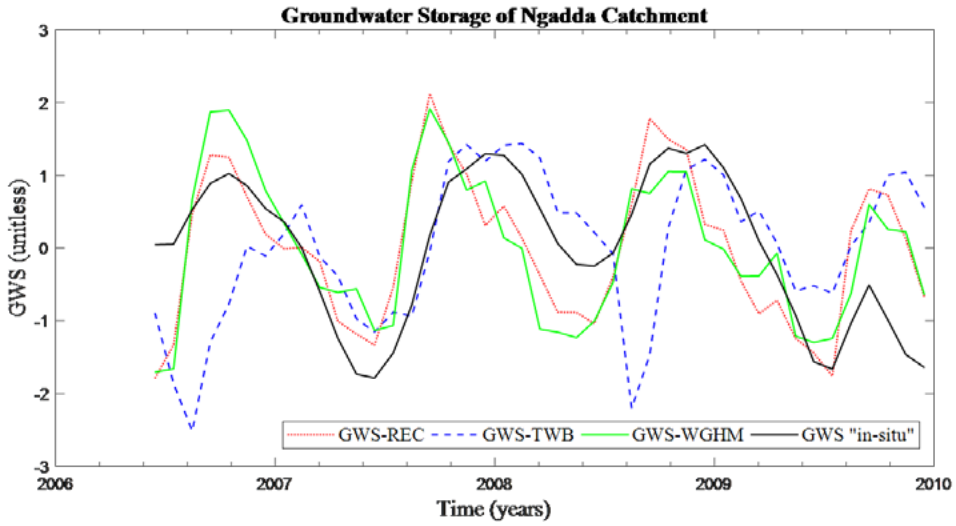

Figure 8: Comparison between the in-situ (solid blackline) and the evaluated GWS series, that is, the reconstructed (red small dashed line), TWS-budget equation (blue dashed line) and WGHM (green solid line) groundwater series.

Figure 8 exhibited the series comparisons established by using statistical indices and it was found that as there was a significant agreement between GRACE-GWS and ground-truth measurements (Table 1).

Table 1: Summary of the comparison between the predicted and observed groundwater time series shown in Figure 8 (they are all unitless since they were normalized by the respective standard deviations of the series).

Indices / Variables	CC (unitless)	STD (unitless)	Mean (unitless)	RMSE (unitless)	NSE (unitless)
GWS-reconstructed	0.60	0.89	0.00	0.89	0.21
GWS-TWS budget	0.28	1.20	0.04	1.20	-0.45
GWS-WGHM	0.56	0.94	0.08	0.94	0.12

Overall, the reconstructed groundwater series for Ngadda catchment performed reasonably better than the GWS retrieved from WGHM hydrological model and GWS obtained from TWS-budget equation. This assumption coincides with the findings reported by Ferreira et al. (2020a) in their study on characterization of hydrogeological regime of Yangzte River Basin.

AUTHOR'S CONTRIBUTION

Author 1: Conceptualization, literature review, methodology, drafting; Author 2: Literature review, methodology; Author 3: Data collection, data analysis; Author 4: Data analysis, editing; Author 5: Writing, revision; Author 6: Revision- writing, final approval.

5. Conclusion

The available remotely sensed and modelled datasets were used to evaluate groundwater storage, and a "tie-in" signal approach was applied to fit the observed TWS from GRACE with its components by applying least-squares, after PCA decomposition for each sub-domain of TWS. The available "in-situ" data were used for validating the GWS results. Therefore, it was found that the surface water extent of Lake Chad presented a slight decrease over the last two decades mostly in the northern part due to the increase in vegetation cover and evaporation. Results from PCA decomposition for each sub-domain of TWS revealed that water storage in LCB is controlled by groundwater and soil moisture, since the surface water seems to be insignificant as explained in the plotted EOFs and PCs of each sub-domain. Furthermore, the reconstructed GWS series for the Ngadda Basin obtained by applying the same procedure as carried out over LCB, WGHM-GWS and TWS-budget GWS were validated against "in-situ" GWS and it was found that as there was a significant agreement between GRACE-GWS and ground-truth measurements. These findings could be of great importance in the planning and management on the use of surface and sub-surface water resources in LCB of Africa.

REFERENCE

Alcamo, J. et al., 2010. Development and testing of the WaterGAP 2 global model of water use and availability. *Hydrological Sciences Journal*, 48, 317–337.

Alla et al., 2019. Application of GRACE to the estimation of groundwater storage change in a data poor region: a case study of Ngadda catchment in the Lake Chad Basin. *Hydrological Processes*, 10, 1–47.

Ayman and Shuanggen, 2014. Water cycle and climate signals in Africa observed by satellite gravimetry[C]. *IOP Conference Series: Earth and Environmental Science*, 17, 1–7.

Baur, O., Kuhn, M., and Featherstone, W.E., 2009. GRACE-derived ice-mass variations over Greenland by accounting for leakage effects, 114, 1–13.

Baur, O. and Sneeuw, N., 2011. Assessing Greenland ice mass loss by means of point-mass modeling: A viable methodology. *Journal of Geodesy*, 85, 607–615.

Bihn et al., 2020. The Lake Chad hydrology under current climate change. *Scientific Reports*, 10, 1–10.

Bonsor and MacDonald, 2011. *An initial estimate of depth to groundwater across Africa*. Website www.bgs.ac.uk Shop online at www.geologyshop.com.

Bormann, I., 2016. Digitizeit: Digitizer software- digitize a scanned graph or chart into (x,y)- data. [online]. Available from: https://www.digitizeit.de/ [Accessed 22 Apr 2020].

Buma and Lee, 2016. Hydrological evaluation of Lake Chad basin using space borne and hydrological model observations. *Water (Switzerland)*, 8, 2–15.

Buma et al., 2018. Recent surface water extent of lake Chad from multispectral sensors and GRACE. *Sensors (Switzerland)*, 18, 1–24.

Döll et al., 2003. A global hydrological model for deriving water availability indicators: Model tuning and validation [J]. *Journal of Hydrology*, 270, 105–134.

Duan X. J.et al., 2009. On the postprocessing removal of correlated errors in GRACE temporal gravity field solutions. *Journal of Geodesy*, 83, 1095–1106.

Famiglietti, 2014. The global groundwater crisis. *Nature Climate Change*, 4, 945–948.

Ferreira et al., 2018. Land water-storage variability over West Africa: Inferences from space-borne sensors. *Water (Switzerland)*, 10, 1–26.

Ferreira et al., 2020a. Characterization of the hydro-geological regime of Yangtze River basin using remotely-sensed and modeled products. *Science of the Total Environment*, 718, 1–44.

Ferreira et al., 2020b. Introducing an improved grace global point-mass solution—a case study in antarctica. *Remote Sensing*, 12 (19), 1–21.

Forootan et al., 2014. Multivariate Prediction of Total Water Storage Changes Over West Africa from Multi-Satellite Data. *Journal of Applied Remote Sensing*, 140, Pages 580-595,.

Forsberg et al., 2017. Greenland and Antarctica Ice Sheet Mass Changes and Effects on Global Sea Level. *Surveys in Geophysics*, 38, 89–104.

Hansen, P.C., 2000. The L-Curve and its Use in the Numerical Treatment of Inverse Problems. *in Computational Inverse Problems in Electrocardiology, ed. P. Johnston, Advances in Computational Bioengineering*, 4, 119–142.

Jacob et al., 2012. Estimating geoid height change in North America: Past, present and future. *Journal of Geodesy*, 86, 337–358.

Jolliffe, I.T., 2000. *Principal Component Analysis(second edition)*. Second edi. Springer Series in Statistics.Springer. New York: I.T.Jolliffe.

Mahdavi-Amiri et al., 2015. Hexagonal connectivity maps for Digital Earth. *International Journal of Digital Earth*, 8, 750–769.

Ndehedehe et al., 2016. Spatio-temporal variability of droughts and terrestrial water storage over Lake Chad Basin using independent component analysis. *Journal of Hydrology*, 540, 106–128.

Odada et al., 2003. *Lake Chad: Agro- Climatic and water balance situation of the Lake Chad basin,*. Experience and lessons learned brief report.

Rodell et al., 2009. Satellite-based estimates of groundwater depletion in India. *Nature*, 460, 999–1002.

S. B. Luthcke et al., 2006. *Recent Greenland Ice Mass Loss by Drainage System from Satellite Gravity Observations.* Scientific Reports.

Schmeer et al., 2012. Separation of mass signals within GRACE monthly gravity field models by means of empirical orthogonal functions. *Journal of Geodynamics*, 59–60, 124–132.

Swenson, S. and Wahr, J., 2006. Post-processing removal of correlated errors in GRACE data. *Geophysical Research Letters*, 33, 1–4.

Tang et al., 2012. Using nonlinear programming to correct leakage and estimate mass change from GRACE observation and its application to Antarctica. *Journal of Geophysical Research B: Solid Earth*, 117, 1–13.

Tregoning et al., 2012. Assessment of GRACE Satellites for Groundwater Estimation in Australia,Waterlines report, National Water Commission [online]. Available from: https://www.researchgate.net/publication/233757174.

Wahr et al., 1998. Time variability of the Earth's gravity field' Hydrological and oceanic effects and their possible detection using GRACE, 103, 205–229.

White et al., 1992. Cartographic and Geometric Components of a Global Sampling Design for Environmental Monitoring. *Cartography and Geographic Information Systems*, 19, 5–22.

Wu, Y., Zhong, B., and Luo, Z., 2018. Investigation of the Tikhonov Regularization Method in Regional Gravity Field Modeling by Poisson Wavelets Radial Basis Functions. *Journal of Earth Science*, 29, 1349–1358.